JOC The Journal of Organic Chemistry

Article

pubs.acs.org/joc

EPR Investigation of Zinc/Iodine Exchange between Propargyl Iodides and Diethylzinc: Detection of Propargyl Radical by Spin Trapping

Julien Maury,[†] Suribabu Jammi,[†] François Vibert,[†] Sylvain R. A. Marque,*[,§] Didier Siri,*[,‡] Laurence Feray,*[,†] and Michèle Bertrand*[,†]

[†]Equipes CMO, [‡]CT, and [§]SREP, Aix-Marseille Université, CNRS, Institut de Chimie Radicalaire UMR 7273, 13397 Cedex 20, Marseille, France

Supporting Information

ABSTRACT: The production of propargyl radicals in the reaction of dialkylzincs with propargyl iodides in nondegassed medium was investigated by EPR using tri-*tert*-butylnitrosobenzene (TTBNB) as a spin trap. The radical mechanism and the nature of the observed species were confirmed by the trapping of propargyl radicals generated by an alternative pathway: i.e., upon irradiation of propargyl iodides in the presence of hexa-*n*-butyldistannane. In dialkylzinc-mediated experiments a high concentration of adduct was instantaneously observed, whereas no spontaneous production of spin adduct was detected in a blank experiment performed with the propargylic iodide and TTBNB in the absence of diethylzinc. Under irradiation in the presence of distannane, two different species were observed at the very beginning of the irradiation; the nitroxide resulting from the trapping of propargyl radical at the propargyl carbon remained the only species detected after irradiating for several minutes. The absence of adducts resulting from the trapping of allenyl canonical forms was supported by DFT calculations and by the preparation of an authentic sample.

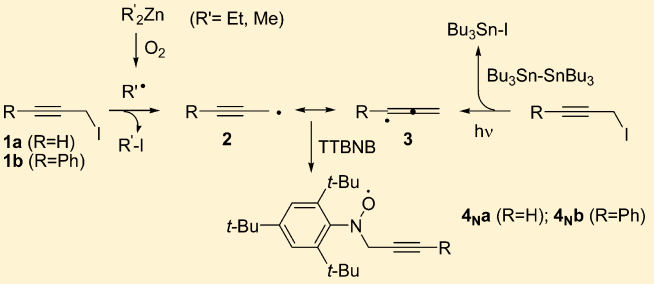

INTRODUCTION

As part of our constant interest in the mechanistic investigation of dialkylzinc reactivity,[1] we recently started studying the mechanism of formation and the reactivity of allenylzinc species. The latter are generally produced from zinc/iodine exchange between propargyl iodides and diethylzinc.[2,3] The chemistry of organic free radicals has experienced a dramatic growth over the last three decades.[4,5] In the family of alkyl radicals, propargyl radical did not raise too much interest, despite the synthetic potential of both acetylenic and allenic linkages. An underlying cause, put forward by Zard, is "the lack of a convenient method for generating them".[6] In the continuity of our previous studies devoted to the use of dialkylzincs as a source of alkyl radicals, it became obvious that the reaction of diethyl- or dimethylzinc with propargyl iodides initiated by oxygen would produce propargyl radicals. EPR experiments, supporting this assertion, are described in this article.

RESULTS AND DISCUSSION

In nondegassed medium the mechanism of zinc/iodine exchange should proceed via the radical chain mechanism shown in Scheme 1. The reaction of diethylzinc with dioxygen is very fast.[7] It results in the formation of ethyl radicals which, due to the strength of the C−I bond in ethyl iodide, undergo iodine atom transfer to produce propargyl radicals.[8,9]

Scheme 1

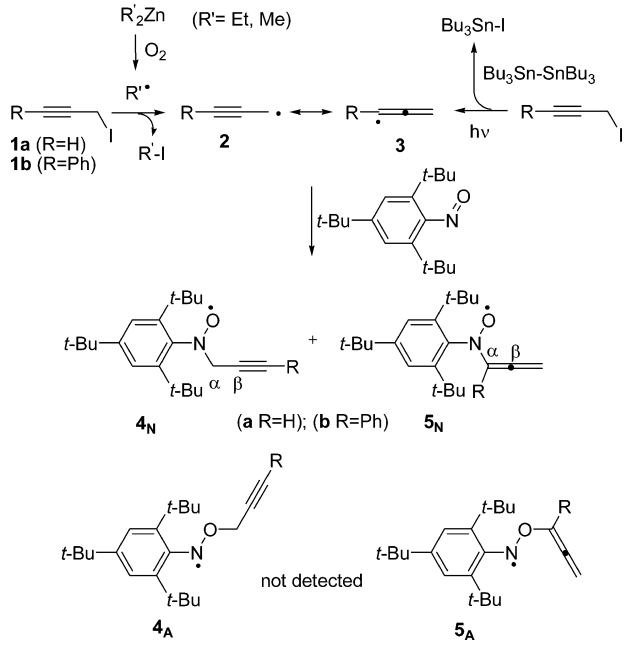

Received: July 27, 2012
Published: September 5, 2012

dx.doi.org/10.1021/jo301562r | J. Org. Chem. 2012, 77, 9081−9086

The spin-trapping approach was the method of choice to probe the formation of propargyl radicals by EPR studies, and tri-*tert*-butylnitrosobenzene (TTBNB) was selected as the spin trap. To the best of our knowledge, no report of any attempt to trap propargyl radicals has ever been reported. Early spectral data regarding the direct observation of propargyl radical in matrixes at low temperature are consistent with a preference for spin localization at the propargyl carbon center.[10] Several authors confirmed this preference from theoretical calculations.[11] However, topological analysis by localization function analysis (ELF) led to the conclusion that propargyl and allenyl resonance canonical forms have equal contributions.[12] Therefore, one would expect that the two canonical forms of propargyl radicals (**2** and **3**) could potentially be trapped to give nitroxides adducts $\mathbf{4_N}$ and $\mathbf{5_N}$ (Scheme 1). It is worth noting that additional trapping leading to anilino radicals $\mathbf{4_A}$ and $\mathbf{5_A}$ could not a priori be ruled out.

Calculations performed at the UB3LYP/6-31+G(d,p) level of theory completed by NRT (natural resonance theory)[13] analysis led to the conclusion that the relative contribution of propargyl and allenyl canonical forms would be 65/35 in the case of skeleton **a** (R = H) and 52:48 in the case of the aryl-substituted radical **b** (R = Ph). Visualizations of the SOMOs of propargyl radicals **2a**,**b** are given in Figure 1. Mulliken spin

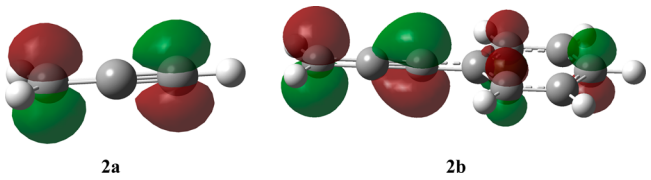

Figure 1. SOMOs of radicals **2a**,**b** calculated at the UB3LYP/6-31+G(d,p) level.

densities at the allenyl and propargyl carbons are 0.6 and 0.91, respectively, in **2a**.[14] Values of 0.51 and 0.76 were calculated for radical **2b**. These values confirm the trend delineated by NRT analysis. Both orbital and steric factors should kinetically favor the trapping at the propargylic carbon.

Generation and Detection of Spin Adducts of Propargyl Radicals. For the sake of simplifying experimental handling, experiments were performed first in nondegassed solvent with TTBNB as the spin trap. Adducts of alkoxy radicals to TTBNB are not persistent at room temperature, and TTBNB is reputedly selective for the trapping of alkyl radicals.[15] Therefore, the trapping of oxygen-centered radicals formed in the initiation step of dialkylzinc-mediated experiments should not interfere with the trapping of carbon-centered species.

Diethylzinc-mediated experiments led to the detection of nitroxyl radicals that were exactly similar to those obtained unambiguously from the production of propargyl radicals via photolysis in the presence of hexa-*n*-butyldistannane (Scheme 1).[16] This is in good agreement with the involvement of a radical pathway in the diethylzinc-mediated formation of allenylzincs.[17] It must be underlined that no spontaneous production of spin adduct was detected in a blank experiment performed with propargylic iodide **1b** and TTBNB in the absence of diethylzinc, in spite of the very low dissociation enthalpy of the C−I bond.[9] The spectra registered from iodides **1a**,**b** are shown in Figures 2 and 3.

Interestingly, in the diethylzinc-mediated reaction, a high concentration of adduct was instantaneously observed, giving

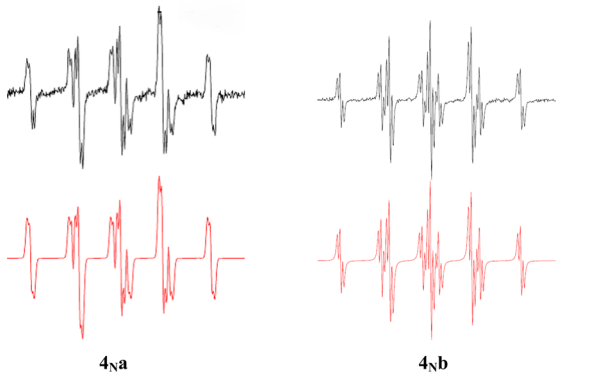

Figure 2. Experimental (upper spectra) and simulated (lower spectra) EPR signals of the spin adducts $\mathbf{4_N}$**a** and $\mathbf{4_N}$**b** recorded at 20 °C, in nondegassed CH_2Cl_2 in the presence of TTBNB as scavenger (5/1 ratio of spin trap to propargyl iodide) and diethylzinc (1 equiv with respect to the iodide).

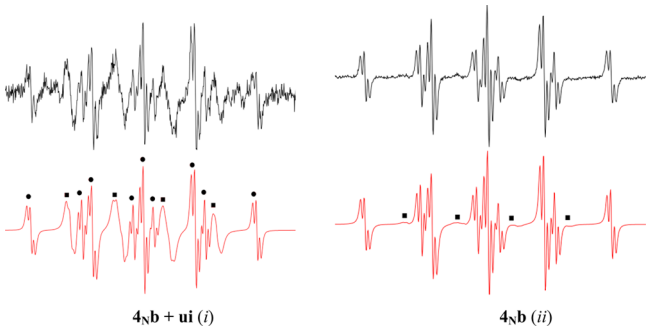

Figure 3. Experimental (upper spectra) and simulated (lower spectra) EPR signals of the spin adducts $\mathbf{4_N}$**b** and an unidentified adduct recorded at 20 °C, in nondegassed CH_2Cl_2 in the presence of TTBNB as scavenger (5/1 ratio of spin trap to propargyl iodide) and *n*-Bu_3SnSn*n*-Bu_3 (1 equiv with respect to the iodide) under irradiation. Legend: (*i*) at the very beginning of the irradiation (● for $\mathbf{4_N}$**b** and ■ for the unidentified species (ui)); (*ii*) after several minutes.

rise to a signal presenting the hyperfine structure of a triplet of triplets of triplets (Figure 2).

When light was used as promoter in the presence of hexa-*n*-butyldistannane, the EPR signal recorded in the early moments of irradiation differed dramatically from that detected after irradiating for several minutes. As exemplified in Figure 3 in the case of **1b**, two species clearly exhibiting different line patterns (typically a triplet of triplets of triplets (●) and something close to a broad quartet (■)) were observed at the very beginning of irradiation (*i*). Whereas the triplet of triplets of triplets signal grew steadily during the irradiation and remained the main signal, after a few minutes only trace amount of the pseudoquartet (pointed by ■) could be detected (*ii*).

It is worth noting that the characteristic pattern of the most abundant detected species is very similar to the pattern of the nitroxide resulting from the trapping of ethyl radical by TTBNB.[18] However, the superimposition of the spectra recorded using either the zinc method or hexa-*n*-butyldistannane under irradiation discarded the possibility of any competitive trapping of ethyl radical in the zinc-mediated experiments. The pattern similarity between ethyl radical spin adduct and the major species resulting from the trapping of propargyl radical led us to conclude that the propargyl canonical form was trapped and that the major species detected from either iodide **1a** or **1b**

dx.doi.org/10.1021/jo301562r | J. Org. Chem. 2012, 77, 9081−9086

were adducts 4_N**a** and 4_N**b**, respectively. None of these patterns corresponded to the expected triplet of ill-resolved triplets signal typical of anilino spin adducts (4_A and 5_A).[19]

It is important to underline that the same adduct was produced irrespective of the nature of the mediator. The fact that dimethylzinc-mediated experiments led to species identical to those produced from diethylzinc[20] is an additional argument to exclude the competitive trapping of ethyl radical.

Comparative experiments were performed under degassed medium. The solution containing **1b** and TTBNB and the solution of diethylzinc were mixed after being degassed separately at 10^{-5} mbar by several cycles of freeze–pump–thaw (see the Supporting Information). After mixing, a signal of 4_N**b** as intense as that in nondegassed medium was observed. This would support the fact that it is almost impossible to prevent trace amounts of oxygen from initiating a radical pathway.[21] Alternatively, the involvement of a single electron transfer (SET) mechanism cannot be excluded.[8]

The different coupling constants a_N, $a_{H\beta}$ (connected to Cα), and a_{Hmeta} (aromatic ring) were determined from the simulations performed with the help of the WinSim 2002 program; they are reported in Table 1. The formed nitroxides

Table 1. Hyperfine Coupling Constants in Nitroxides 4_N

	a_N (G)	$a_{H\beta}$ (G)	a_{Hmeta} (G)	ΔH_{pp} (G)
4_N**a**	13.39	15.51[a]	0.85	0.45
4_N**b**	13.42	16.09[a]	0.85	0.42

[a]The two hydrogens in β-positions exhibit identical coupling constants.

exhibited two identically coupled β-hydrogen nuclei with an $a_{H\beta}$ value of 15.51 G in the case of 4_N**a** and an $a_{H\beta}$ value of 16.09 G in the case of 4_N**b**. The a_N values were 13.39 and 13.42 G, respectively (g = 2.0059, 0.42–0.45 G line width (ΔH_{pp})). We have recently reported a $a_{H\beta}$ value of 17.50 G for the two equivalent β-hydrogens of the ethyl radical spin adduct to TTBNB in hexane[17,22,23] (blank experiments performed with Et_2Zn and TTBNB, in the absence of iodide, in dichloromethane led to an ethyl radical adduct having a_N, $a_{H\beta}$, and a_{Hmeta} values of 13.58, 18.10, and 0.83 G, respectively; see the Supporting Information).

However, the conclusion that propargyl radicals would be trapped at the propargyl carbon might be too hasty, since the two terminal hydrogen nuclei in nitroxide 5_N might exhibit high a_H coupling constants. This should be a consequence of the overlap of the allenyl π-system with the p orbital describing the odd electron at nitrogen, which induces delocalization of spin density to the central carbon atom in the allene moiety and the terminal hydrogens (Figure 4). Conversely, when R = H, due to the 90° dihedral angle, the $a_{H\beta}$ coupling constant should be close to 0 for the hydrogen located at Cα in the allene moiety.[24,25]

A a_N value of 13.7 G and a completely different $a_{H\beta}$ value of 2.3 G have been reported for nitroxyl radical **6** (eq 1). The alkynyl radical adduct with *N*-*tert*-butyl-α-phenyl nitrone was generated from the reaction of $M(CO)_6$ complexes with

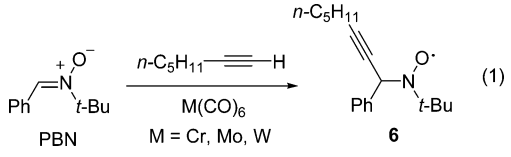

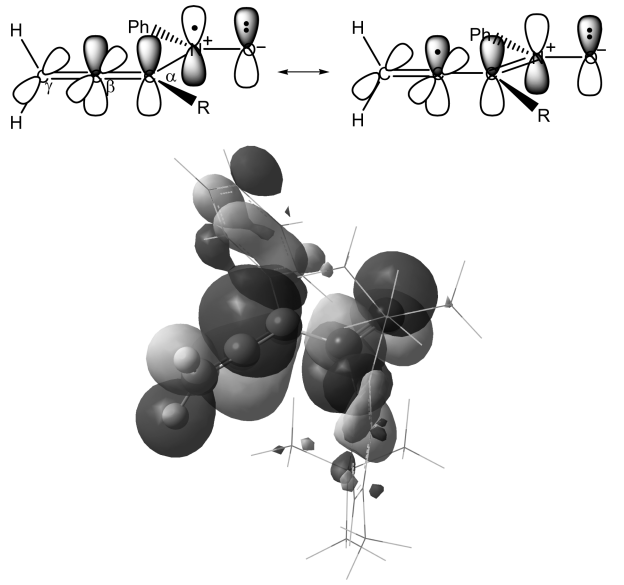

Figure 4. (top) Spin delocalization in allenyl nitroxides 5_N (R = H, Ph) and (bottom) 5_N**b** SOMO symmetry.

1-heptyne in the presence of PBN.[26] This very different $a_{H\beta}$ value should be the consequence of steric interactions, leading to a preferential conformation of **6**, where the hydrogen would lie close to the plane of the nitroxyl group.

Therefore, DFT calculations were used to determine the preferred conformations of radicals 4_N and 5_N. For the sake of saving time, calculations were performed on analogous nitroxides bearing a methyl group instead of a *tert*-butyl group at the para position on the aromatic ring. The geometries were optimized by the M06-2X method using the 6-31G(d) basis set.[27] Coupling constants were calculated by the PBE0/6-31+G(d)//M06-2X/6-31G(d) method.[28] Mulliken spin density populations at nitrogen, oxygen, and carbon atoms and theoretical values of hyperfine coupling constants (hfcc) are given in Table 2.

The most stable conformations of radicals 4_N and 5_N are all symmetrical. They are shown in Figure 5.

The average dihedral angle (θ) between the p orbital at nitrogen describing the odd electron and the vicinal C–H bonds is 33° in both 4_N**a** and 4_N**b**. These dihedral angles are quite similar to those observed in the preferred conformation of ethyl radical adduct. According to the Heller–McConnell relationship,[23,24] this accounts for two β-hydrogens exhibiting identical a_H values, and these conformers give a good approximation for the hydrogen hfcc (Table 2).

As shown in Figure 6, the variation of the dihedral angle (40° of amplitude) around the equilibrium position was shown to have little incidence on the electronic energy of radical 4_N**a** (less than 3 kJ mol^{-1}). Therefore, the values of $a_{H\beta}$ fluctuate freely within the limits of 11.9 and 18.5 G.

It must be underlined that, according to the most stable conformations of model nitroxides 5_N shown in Figure 5, calculations predict that the two equivalent allenyl protons would exhibit $a_{H\beta}$ coupling constants of 17.2 and 17.5/16.7 G in 5_N**a** and 5_N**b**, respectively. However, the partial delocalization of spin density at the central carbon of the allene moiety should decrease the spin density at nitrogen. As a consequence, the a_N coupling constant should be much lower in 5_N than in 4_N.

The calculations did not give theoretical values of a_N close to the experimental values. The calculated values are generally

dx.doi.org/10.1021/jo301562r | J. Org. Chem. 2012, 77, 9081–9086

Table 2. Hyperfine Coupling Constants and Mulliken Spin Density Populations (Electrons) Calculated by the PBE0/6-31+G(d) Method on Geometries Optimized at the M06-2X/6-31G(d) Level of Theory

	hyperfine coupling constant			Mulliken spin density			
nitroxyl radical	a_N (G)	$a_{H\beta}$ (G)	a_{Hmeta} (G)	N$^\bullet$	O$^\bullet$	C$_\alpha^\bullet$	C$_\beta^\bullet$
$\mathbf{4_N a}$	11.3	16.6	0.8	0.45	0.50	−0.07	0.02
$\mathbf{4_N b}$	11.4	16.5	0.8	0.46	0.49	−0.08	0.02
$\mathbf{5_N a}$	9.5	17.2	0.6	0.38	0.47	−0.18	0.34
$\mathbf{5_N b}$	10.3	17.5/16.7	0.7/0.5	0.37	0.47	−0.15	0.32

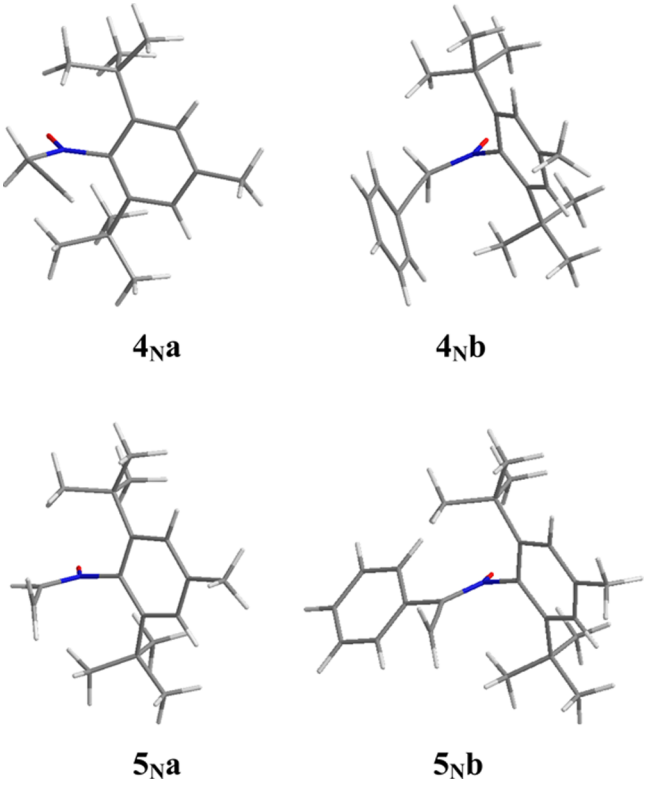

Figure 5. Stereoviews of the most stable conformers of $\mathbf{4_N}$ and $\mathbf{5_N}$.

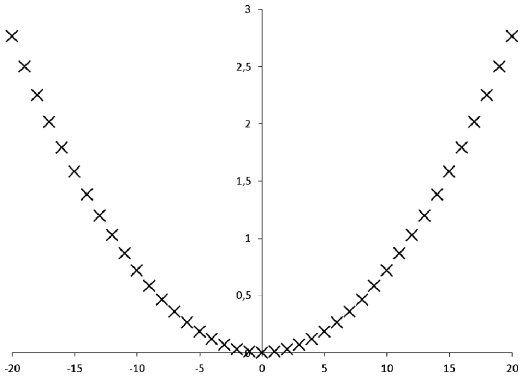

Figure 6. Fluctuation of electronic energy of $\mathbf{4_N a}$, calculated at the M06-2X/6-31G(d) level, around the equilibrium value of the θ dihedral angle.

underestimated with respect to the experimental values,[27] but the trapping of propargyl radicals at the propargylic carbon fits better with both a_N and $a_{H\beta}$ experimental values.[29]

Model $\mathbf{5_N}$ radical species are more stable than $\mathbf{4_N}$ isomeric forms. According to DFT calculations, refined at the M06-2X/6-311++G(3df,3pd)//M06-2X/6-31G(d) level of theory in order to get accurate comparative energy values,[26] the model for nitroxyl radical $\mathbf{5_N a}$ would be more stable by 31 kJ mol^{-1} than $\mathbf{4_N a}$ and the model for nitroxyl radical $\mathbf{5_N b}$ would be more stable by 16 kJ mol^{-1} than $\mathbf{4_N b}$. The detection of propargylic nitroxides $\mathbf{4_N}$ would result from kinetic control. This is in agreement with the respective weight of propargyl and allenyl canonical forms. However, this interpretation should be taken cautiously, since nothing is known about the persistence of allenyl or even vinyl nitroxides.

In order to confirm this assumption, the reaction profiles of the two competitive addition paths to TTBNB were calculated. The transition states were located and confirmed by the intrinsic reaction coordinate (IRC) approach; their energies were determined at the M06-2X/6-311++G(3df,3pd)//M06-2X/6-31G(d) level of theory (Figure 7). As expected for highly

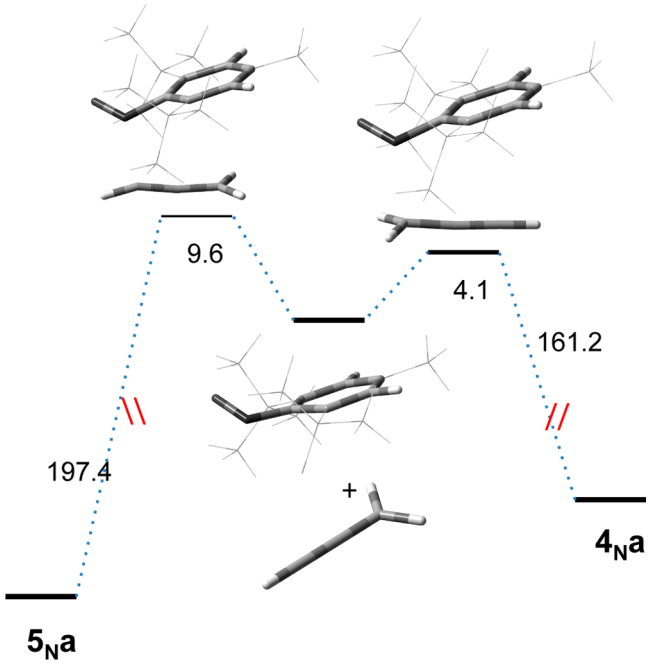

Figure 7. Activation energies (kJ mol^{-1}) for the trapping of allenyl and propargyl canonical forms of radical **2a** (M06-2X/6-311++G-(3df,3pd)//M06−2X/6-31G(d) level).

exothermic reactions, both transition states are very early. The C−N distances are 2.36 and 2.29 Å in the transition states leading to $\mathbf{4_N a}$ and $\mathbf{5_N a}$, respectively. Comparatively, C−N bond lengths are 1.48 and 1.40 Å in $\mathbf{4_N a}$ and $\mathbf{5_N a}$, respectively. The activation barrier for the radical trapping leading to $\mathbf{4_N a}$ is lower than that of the path leading to $\mathbf{5_N a}$ by 5.5 kJ mol^{-1}. As a consequence, the rate constant for the former pathway would be 1 order of magnitude higher than the rate constant for the latter pathway.

Eventually, in order to assess unambiguously which canonical form of propargyl radical was effectively trapped, attempts to

dx.doi.org/10.1021/jo301562r | J. Org. Chem. 2012, 77, 9081−9086

prepare an authentic sample of 4_N**a** from amine **7a** according to eq 2 were achieved by oxidation with *m*-CPBA directly in the

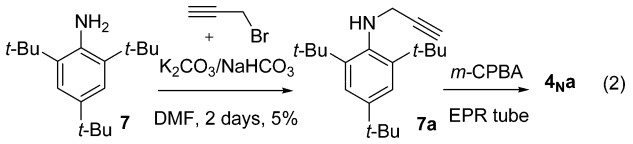

(2)

EPR tube.[30] Due to the low basicity of the nitrogen atom and to steric hindrance, the overall yield in the alkylation of **7** was very low, but the prepared quantity was sufficient for the spectroscopic experiment to be achieved.

No ambiguity resulted from the latter experiment, which led to a spectrum which could be superimposed on that assigned to 4_N**a**.[31]

In conclusion, by carrying out EPR experiments using different experimental approaches, it was possible to get evidence for the trapping of propargyl radicals at the propargylic carbon atom. A theoretical approach using DFT calculations might be considered as equivocal on the grounds of the calculated $a_{H\beta}$ coupling constants. However, both calculated $a_{H\beta}$ and a_N coupling constant values fit better with the trapping of the propargyl canonical form and confirm the assignment. This work supports the proposal of a radical chain mechanism for the reaction of propargyl iodides with diethylzinc, leading to allenylzinc species in nondegassed medium. A radical mechanism is in all likelihood operative in the formation of allenylzincs even in degassed medium, as it is difficult to exclude traces of dioxygen by thoroughly degassing solutions.

EXPERIMENTAL SECTION

EPR experiments were performed with commercially available HPLC grade solvents and reactants, which were used as received. EPR experiments were performed on an ELEXSYS Bruker instrument. The photolysis instrument (ORIEL version 66901 with an energy supplier version 68911) is equipped with a 300X UXL306 arc Xe lamp (300−2400 nm) with an optical fiber (1 m, version 77620). EPR spectra were simulated using WinSim 2002 software.

2,4,6-Tri-*tert*-butyl-*N*-(prop-2-yn-1-yl)aniline (7a; CAS Registry No. 132588-88-6). A mixture of 2,4,6-tri-*tert*-butylphenylamine (100 mg, 1 equiv), potassium carbonate (52.4 mg, 1 equiv), and sodium bicarbonate (31.9 mg, 1 equiv) in DMF (3 mL) was heated at 100 °C and stirred for 10 min. To this mixture was slowly added propargyl bromide (89 mg, 2 equiv) in DMF (1 mL), and the resulting mixture was stirred at 100 °C for 2 days. The reaction mixture was poured into ether and then washed with water and brine. The organic layer was dried over magnesium sulfate and filtered, and the solvent was removed under reduced pressure. The residue was purified by flash column chromatography (Et_2O/pentane, 5/95) to obtain 2,4,6-tri-*tert*-butyl-*N*-(prop-2-yn-1-yl)aniline (**7a**) in 5% yield as a sticky oil. ^{1}H NMR (400 MHz, $CDCl_3$): δ 7.20 (s, 2H), 3.46 (d, J = 2.5 Hz, 2H), 3.23 (br s, 1H), 2.21 (t, J = 2.5 Hz, 1H), 1.41 (s, 18H), 1.22 (s, 9H). ^{13}C NMR (100 MHz, $CDCl_3$): δ 144.2, 144.9, 144.0, 123.4, 82.1, 71.6, 42.9, 36.6, 34.8, 32.8, 31.7. HRMS: calcd for $C_{21}H_{34}N^+$ $(M + H)^+$ 300.2686, found 300.2685.

General Procedures for the Recording of EPR Spectra. EPR experiments were performed in undegassed CH_2Cl_2 as solvent under each of the following conditions: 0.1 mL (0.01 mmol) of a 0.1 M solution of dialkylzinc in hexane (or heptane) was added to a mixture of TTBNB and propargyl iodide (0.05/0.01 mmol) in dichloromethane (0.24 mL) at room temperature; 0.1 mL (0.005 mmol) of a 0.05 M solution of $(Bu_3Sn)_2$ in dichloromethane was added at room temperature to a solution containing TTBNB and the propargyl iodide (0.05/0.01 mmol) in dichloromethane (0.24 mL).

Computational Details. All the calculations were performed with the Gaussian 09 package.[32] The geometries were fully optimized at the M06-2X/6-31G(d) level of theory. Vibrational frequencies were calculated at the M06-2X/6-31G(d) level to determine the nature of the calculated geometries (0 imaginary frequencies for minima, 1 imaginary frequency for TS). Zero-point energies and thermodynamic data were calculated using the specified scale factor (0.947).[33] Single-point energies were performed at the PBE0/6-31+G(d) level to calculate hyperfine coupling constants. As shown by Houriez et al.,[34] this level of theory is enough to provide accurate hyperfine coupling constants. More accurate single-point energies were determined at the M06-2X/6-311++G(3df,3pd)//M06-2X/6-31G(d) level to compare the stabilities of the different propargyl/allenyl nitroxyl and anilino adducts.

ASSOCIATED CONTENT

Supporting Information

Text, figures, and tables giving EPR spectra, details of the synthesis and NMR spectra of amine **7a**, and computational details. This material is available free of charge via the Internet at http://pubs.acs.org.

AUTHOR INFORMATION

Corresponding Author

*E-mail: michele.bertrand@univ-amu.fr (M.B.); laurence.feray@univ-amu.fr (L.F.); sylvain.marque@univ-amu.fr (S.R.A.M.); didier.siri@univ-amu.fr (D.S.).

Notes

The authors declare no competing financial interest.

REFERENCES

(1) For review on dialkylzincs in radical chemistry, see: (a) Bazin, S.; Feray, L.; Bertrand, M. P. *Chimia* **2006**, *60*, 260−265. For recent reports on the subject see also: (b) Maury, J.; Feray, L.; Perfetti, P.; Bertrand, M. P. *Org. Lett.* **2010**, *12*, 3590−3593. (c) Maury, J.; Feray, L.; Bertrand, M. P. *Org. Lett.* **2011**, *13*, 1884−1887. (d) Maury, J.; Mouysset, D.; Feray, L.; Marque, S. R. A.; Siri, D.; Bertrand, M. P. *Chem. Eur. J.* **2012**, *18*, 3241−3247. (e) Akindele, T.; Yamada, K.-I.; Tomioka, K. *Acc. Chem. Res.* **2009**, *42*, 345−355.

(2) For reviews, see: (a) Marshall, J. A.; Gung, B. W.; Grachan, M. L. Synthesis and Reactions of Allenyl Compounds; In *Modern Allene Chemistry*; Krause, N., Hashmi, A. S. K., Eds.; Wiley-VCH: Weinheim, Germany, 2004; pp 493−592. (b) Marshall, J. A. In *The Chemistry of Organozinc Compounds*; Rappoport, Z., Marek, I., Eds.; Wiley: New York, 2006, Vol. *1*, pp 421−455. (c) Botuha, C.; Chemla, F.; Ferreira, F.; Pérez-Luna, A.; Roy, B. *New. J. Chem.* **2007**, *31*, 1552−1567. For the propargylation of imines, see also: (d) Botuha, C.; Chemla, F.; Ferreira, F.; Louvel, J.; Pérez-Luna, A. *Tetrahedron: Asymmetry* **2010**, *21*, 1147−1153 and previous references cited therein.

(3) Trost, B. M.; Ngai, M.-Y.; Dong, G. *Org. Lett.* **2011**, *13*, 1900−1903.

(4) *Radicals in Organic Synthesis*; Renaud, P., Sibi, M., Eds.; Wiley-VCH: Weinheim, Germany, 2001, Vols. *I* and *II*.

(5) *Encyclopedia of Radicals in Chemistry, Biology and Materials*; Chatgilialoglu, C., Studer, A., Eds.; Verlag: Weinheim, Germany, 2012.

(6) Alameda-Angulo, C.; Quiclet-Sire, B.; Zard, S. Z. *Tetrahedron Lett.* **2006**, *47*, 913−916.

(7) Seyferth, D. *Organometallics* **2001**, *20*, 2940−2955 and previous references therein.

(8) The formation of alkyl radicals could also be promoted by single electron transfer from Et_2Zn to the alkyl iodide. For the proposal of a single electron transfer mechanism in reactions involving dialkylzincs, see: Kaupp, M.; Stoll, H.; Preuss, H.; Kaim, W.; Stahl, T.; Van Koten, G.; Wissing, E.; Smeets, W. J. J.; Spek, A. L. *J. Am. Chem. Soc.* **1991**, *113*, 5606−5618. Indeed, under an inert atmosphere, zinc/iodine exchange has already been exploited as a source of allenylzinc species and a radical chain mechanism might similarly be operative under these experimental conditions.

(9) The experimental values for the C−I bond dissociation enthalpy are 233.5 kJ mol^{-1} in ethyl iodide and 184.6 kJ mol^{-1} in 3-iodoprop-1-yne; see *Handbook of Bond Dissociation Energies in Organic Compounds*; Luo, Y.-R., Ed.; CRC Press: Boca Raton, FL, 2007.
(10) (a) Kasai, P. H. *J. Am. Chem. Soc.* **1972**, *94*, 5950−5956. (b) Collin, J.; Lossing, F. P. *J. Am. Chem. Soc.* **1957**, *79*, 5848−5853. (c) Kochi, J. K.; Krusic, P. J. *J. Am. Chem. Soc.* **1970**, *92*, 4110−4114. (d) For indirect additional studies, see: Adam, W.; Ortega-Schulte, C. M. *J. Org. Chem.* **2003**, *68*, 1007−1011.
(11) (a) Benson, H. G.; Bowles, A. J.; Hudson, A.; Jackson, R. A. *Mol. Phys.* **1971**, *21*, 713−719. (b) Rogers, D. W.; Matsunaga, N.; Zavitsas, A. A. *J. Org. Chem.* **2006**, *71*, 2214−2219.
(12) Krokidis, X.; Moriarty, N. W.; Lester, W. A., Jr.; Frenklach., M. *Chem. Phys. Lett.* **1999**, *314*, 534−542.
(13) (a) Glendening, E. D.; Weinhold, F. *J. Comput. Chem.* **1998**, *19*, 593−609. (b) Glendening, E. D.; Weinhold, F. *J. Comput. Chem.* **1998**, *19*, 610−627. (c) Glendening, E. D.; Badenhoop, J. K.; Weinhold, F. *J. Comput. Chem.* **1998**, *19*, 628−646.
(14) More accurate calculations at the M06-2X/6-311++G(3df,3pd)//M06-2X/6-31G(d) level led to an increased gap between the spin densities 0.51 and 1.09 at the allenyl and propargyl centers, respectively.
(15) (a) Terabe, S.; Konaka, R. *J. Chem. Soc., Perkin Trans. 2* **1973**, 369−374. (b) Mekarbane, P. G.; Tabner, B. J. *Magn. Reson. Chem.* **1998**, *36*, 826−832. (c) Mekarbane, P. G.; Tabner, B. J. *Magn. Reson. Chem.* **2000**, *38*, 845−852.
(16) Curran, D. P.; Kim, D. *Tetrahedron* **1991**, *47*, 6171−6188.
(17) Other data supporting the radical mechanism and the influence of oxygen on the formation of allenylzincs from propargyl iodides and diethylzinc will be published in a forthcoming article.
(18) Maury, J.; Feray, L.; Bazin, S.; Clément, J.-L.; Marque, S. R. A.; Siri, D.; Bertrand, M. P. *Chem. Eur. J.* **2011**, *17*, 1586−1595.
(19) Anilino radicals have *g* values lower than those of nitroxyl radicals (2.0036−2.0040/2.0058−2.0060) and typical a_N and $a_{H\beta}$ coupling constants of 11.6 and 2.1 G, respectively. None of these characteristic signals were observed. This means that such species are not present in an amount significant enough to be assessed with reliability. See ref 15 and: (a) Mekarbane, P. G.; Tabner, B. J. *J. Chem. Soc., Perkin Trans. 2* **2000**, 1465−1470. (b) Konaka, R.; Terabe, S. *J. Am. Chem. Soc.* **1971**, *93*, 4306−4307.
(20) In contrast to what happens in the case of diethylzinc, an allenylzinc species cannot be generated in the case of dimethylzinc. Propargyl radicals could be formed from the transfer of the propargylic iodine atom to either methyl or ethyl radical, whereas, owing to the fact that the C−Zn bond is much stronger in dimethylzinc than in diethylzinc (see ref 17), subsequent homolytic substitution at zinc cannot proceed in the case of dimethylzinc. Even though the iodine atom transfer is more exothermic in the case of the methyl radical than in the case of the ethyl radical, the overall two-step process is not exothermic enough to be efficient.
(21) Ethyl radical was similarly trapped in blank experiments where the diethylzinc solution and the solution containing TTBNB were mixed after being degassed, in separate compartments, by several cycles of freeze−pump−thaw.
(22) For pioneering investigations by EPR of the reaction of dialkylzincs with *tert*-butoxy radical, see: (a) Davies, A. G.; Roberts, B. P. *J. Chem. Soc. B* **1968**, 1074−1078. (b) Davies, A. G.; Griller, D.; Roberts, B. P. *J. Chem. Soc. B* **1971**, 1823−1829. (c) Davies, A. G.; Roberts, B. P. *Acc. Chem. Res.* **1972**, 387−392.
(23) For other spin-trapping experiments involving dimethylzinc, see: Mileo, E.; Benfatti, F.; Cozzi, P. G.; Lucarini, M. *Chem. Commun.* **2009**, 469−470.
(24) Gerson, F.; Huber, W. *Electron Spin Resonance Spectroscopy of Organic Radicals*; Wiley-VCH: Weinheim, Germany, 2003.
(25) Janzen, E. G.; Coulter, G. A.; Oehler, U. M.; Bergsma, J. P. *Can. J. Chem.* **1982**, *60*, 2725−2733.
(26) Hwang, J. S.; Tsonis, C. P. *React. Kinet. Catal. Lett.* **1994**, *52*, 347−356.
(27) (a) Zhao, Y.; Truhlar, D. G. *Theor. Chem. Acc.* **2008**, *120*, 215−241. (b) Hohenstein, E. G.; Chill, S. T.; Sherill, C. D. *J. Chem. Theory Comput.* **2008**, *4*, 1996−2000. (c) Bryantsev, V. S.; Diallo, M. S.; van Duin, A. C. T.; Goddard, W. A., III *J. Chem. Theory Comput.* **2009**, *5*, 1016−1026.
(28) Improta, R.; Barone, V. *Chem. Rev.* **2004**, *104*, 1231−1254.
(29) Calculations of hyperfine coupling constants in anilino radicals $\mathbf{5_A b}$ led to the following values: a_N = 12.1 G, a_H = 4.1 and 3.7 G (terminal methylene group), a_{Hmeta} = 3.0 and 3.3 G. Calculations of hyperfine coupling constants in anilino radicals $\mathbf{4_A b}$ led to the following values: a_N = 16.4 G, a_H= −0.4 and 3.1 G (propargylic methylene group), a_{Hmeta} = 1.4 and 1.4 G. No related hyperfine structure could be detected in the recorded spectra. According to theoretical calculations, $\mathbf{5_A a}$ was found to be more stable than $\mathbf{4_A a}$ by 14.6 kJ mol^{-1}. However, $\mathbf{5_A b}$ was found to be less stable than $\mathbf{4_A b}$ by 5.4 kJ mol^{-1}.
(30) The procedure already described by Barmettler et al. was reproduced for the synthesis of amine **7a** (HMPA was replaced by DMF); see: Barmettler, P.; Hansen, H.-J. *Helv. Chim. Acta* **1990**, *73*, 1515−1573.
(31) The resolution (ΔH_{pp} = 0.95) was, however, much lower than in the case of the experiments performed from propargyl iodide (see the Supporting Information).
(32) Frisch, M. J.; Trucks, G. W.; Schlegel, H. B.; Scuseria, G. E.; Robb, M. A.; Cheeseman, J. R.; Scalmani, G.; Barone, V.; Mennucci, B.; Petersson, G. A.; Nakatsuji, H.; Caricato, M.; Li, X.; Hratchian, H. P.; Izmaylov, A. F.; Bloino, J.; Zheng, G.; Sonnenberg, J. L.; Hada, M.; Ehara, M.; Toyota, K.; Fukuda, R.; Hasegawa, J.; Ishida, M.; Nakajima, T.; Honda, Y.; Kitao, O.; Nakai, H.; Vreven, T.; Montgomery, J. A., Jr.; Peralta, J. E.; Ogliaro, F.; Bearpark, M.; Heyd, J. J.; Brothers, E.; Kudin, K. N.; Staroverov, V. N.; Kobayashi, R.; Normand, J.; Raghavachari, K.; Rendell, A.; Burant, J. C.; Iyengar, S. S.; Tomasi, J.; Cossi, M.; Rega, N.; Millam, J. M.; Klene, M.; Knox, J. E.; Cross, J. B.; Bakken, V.; Adamo, C.; Jaramillo, J.; Gomperts, R.; Stratmann, R. E.; Yazyev, O.; Austin, A. J.; Cammi, R.; Pomelli, C.; Ochterski, J. W.; Martin, R. L.; Morokuma, K.; Zakrzewski, V. G.; Voth, G. A.; Salvador, P.; Dannenberg, J. J.; Dapprich, S.; Daniels, A. D.; Farkas, Ö.; Foresman, J. B.; Ortiz, J. V.; Cioslowski, J.; Fox, D. J. *Gaussian 09, Revision A.02*; Gaussian, Inc., Wallingford CT, 2009.
(33) NIST Computational Chemistry Comparison and Benchmark Database. NIST Standard Reference Database Number 101. Release 15b, August 2011, Editor: Russell D. Johnson III. http://cccbdb.nist.gov/.
(34) Houriez, C.; Ferre, N.; Siri, D.; Tordo, P.; Masella, M. *J. Phys. Chem. B* **2010**, *114*, 11793−11803.